G. W. Brodland
Departments of Civil Engineering and Biology,
University of Waterloo,
Waterloo, ON
N2L 3G1
Mem. ASME

D. A. Clausi
Department of Systems Design Engineering,
University of Waterloo,
Waterloo, ON
N2L 3G1

Embryonic Tissue Morphogenesis Modeled by FEM

A three-dimensional, large-strain finite element formulation for the simulation of morphogenetic behaviors in embryonic tissues is presented. It is used to investigate aspects of invagination, neural tube morphogenesis, contraction wave propagation and mechanical pattern formation. The simulations show that the spacing of patterns and the shapes produced by certain morphogenetic movements in epithelial sheets depend only slightly on the properties of the materials which underlie these sheets. Simulations of neural tube closure show that numerous, experimentally-observed features can be produced by contraction of apical microfilament bundles alone. That certain systems of forces are mechanically equivalent and that certain patterns of deformations are equivalent set practical limits on what can be inferred from the simulations.

Introduction

A variety of intriguing processes are critical to early embryogenesis (Alberts et al., 1989). Observers have, for millennia, attempted to identify the essential phenomena responsible for each of these processes. Although it is known that electrical, biochemical, and mechanical phenomena can be involved, the specific causes of many embryonic processes which seem elementary are still unknown.

Mathematical models and computer simulations which complement physical experiments have been important to the testing of hypotheses about the forces and other factors which drive morphogenetic processes. Specifically, they have helped distinguish between factors which are causal and those which are not. Computer simulations have also demonstrated the relationship between local and global shape changes (Jacobson and Gordon, 1976; Hilfer and Hilfer, 1983) and confirmed hypotheses about the forces required to produce observed shape changes (Odell et al., 1981; Weliky and Oster, 1990; Dunnett et al., 1991; Clausi, 1991; Clausi and Brodland, 1993). These studies have firmly established computer simulations as a scientific tool for the study of morphogenetic processes.

At the same time these studies have made us aware of the need for additional and more detailed simulations (Jacobson, 1980; Albrecht-Buehler, 1990; Koehl, 1990). Koehl writes ". . .it is critical that we complement the popular molecular and biochemical approaches to the control of morphogenesis with nuts-and-bolts analyses of the physics of how morphogenetic processes occur."

Here, a set of criteria is presented for the modeling of morphogenetic mechanical behaviors in embryonic tissue. The essential features of a finite element formulation which satisfies these criteria is outlined. The formulation is then used to demonstrate how mechanical interactions can give rise to a variety of biological phenomena. Aspects of tissue invagination, neural tube formation, mechanical pattern formation, and contraction wave propagation are investigated.

What Drives Morphogenetic Movements?

Many morphogenetic movements are driven by forces produced in the epithelium, the outer-most layer of tissue. These forces are typically generated by cytoskeletal components and by various kinds of inter-cellular forces. Considerable debate continues about the possible involvement of other force generators and about the role of subjacent tissue layers in specific morphogenetic processes. Various lines of evidence, including finite element simulations, however, suggest that many morphogenetic shape changes are driven by cytoskeletal components, especially microfilaments, in the epithelial layer (Clausi and Brodland, 1993).

Typical components of an epithelial cell sheet which may be of mechanical importance are shown in Fig. 1. To quantitate the mechanical properties of substructural components such as microfilaments, microtubules, cytoplasm and other structures is difficult, at best. *In vivo*, these components are subject to complex mechanical interactions with other components and with other cells, and their mechanical behavior can be highly dependent on biomechanical factors (Nakamura and Hira-

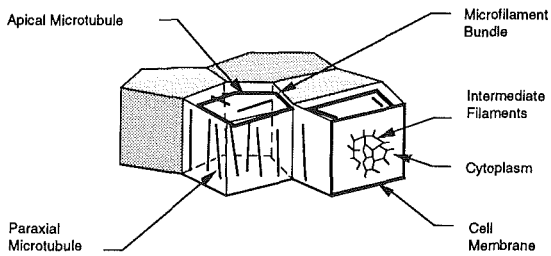

Fig. 1 Sub-cellular components which may be of mechanical importance

Contributed by the Bioengineering Division for publication in the JOURNAL OF BIOMECHANICAL ENGINEERING. Manuscript received by the Bioengineering Division July 14, 1992; revised manuscript received July 6, 1993. Associate Technical Editor: R. M. Hochmuth.

moto, 1978; Cassimeris et al., 1988; Alberts et al., 1989). The small size of these components further complicates measurement of their properties.

Microfilaments. The existence and contractile nature of circumferential bundles of microfilaments at the apical end of epithelial cells is now well established (Rappaport, 1977; Gordon and Brodland, 1987; Gordon and Essner, 1987). Fluorescence studies (Lee and Nagele, 1985) support the hypothesis of Burnside (1971, 1973) that the actin and myosin components of microfilaments intercalate as they shorten so that microfilament volume remains constant. Since the contractile stress, σ, apparently remains constant, the force exerted by a microfilament increases as it shortens (Rappaport, 1977; Gordon and Brodland, 1987). We model this phenomenon using the equation

$$f = \sigma A_0 \frac{L_0}{L}, \tag{1}$$

where A_0 is the cross-sectional area in a reference configuration, L_0 and L, are the reference and current lengths, L_0 and L.

At rest, these filamentous components exert a constant tensile stress, called a tonus. When a stretch activated contraction occurs, they exert a much stronger tensile force (Gordon and Brodland, 1987). Initiation of stretch-activated contractions appears to involve the cell membrane (Stephens, 1984; Regirer, 1989; Sachs, 1990).

Microtubules. Microtubules are another ubiquitous cytoskeletal component (Dustin, 1984). Theoretical models of microfilament force generation have been proposed by Hill, Kirshner and others (Hill, 1981; Hill and Kirshner, 1982a, b). Recent experimental evidence has supported many of the predictions of these models including some of the transient characteristics of microtubules (Horio and Hotani, 1986). The flexural properties of microtubules have also been measured (Mizushima-Sugano et al., 1983) and their interaction with other cytoskeletal components identified (Brodland and Gordon, 1990).

Cytoplasm and Intermediate Filament Networks. The mechanical properties of cytoplasm have been investigated by a variety of intriguing methods (Hiramoto, 1969a, b; Valberg and Alvertini, 1985). In general, these tests measure viscoelastic properties over a period of a few seconds, a rather short duration compared to the hours required for cell sheet shape changes. In addition, the strain rates used in these tests are magnitudes higher than those which occur during morphogenesis. Available estimates of cytoplasmic properties likely involve tearing of the intermediate filament meshwork which courses through the cells (Brodland and Gordon, 1990) and therefore seem not to be directly applicable to studies of gradual morphogenetic movements. It is likely that significant remodeling by depolymerization and repolymerization occurs in many of the cytoskeletal components, including intermediate filaments, during the time course of interest here. We follow the approach of Brodland and Gordon (1990) and represent the cytoplasm, including any intermediate filament mesh which might be present, as an isotropic viscoelastic material.

Other Force Generators. At least two kinds of forces which might influence morphogenetic shape changes are produced within the cell membrane. The first of these is intercellular forces which result from the mechanical stiffness of the cell membrane (Alberts et al., 1989). The second results from intracellular adhesions. Computer models have shown that intracellular adhesions could drive morphogenetic movements (Weliky and Oster, 1990). Other computer studies have suggested that the effect of such adhesions may be less significant than once thought (Clausi and Brodland, 1993).

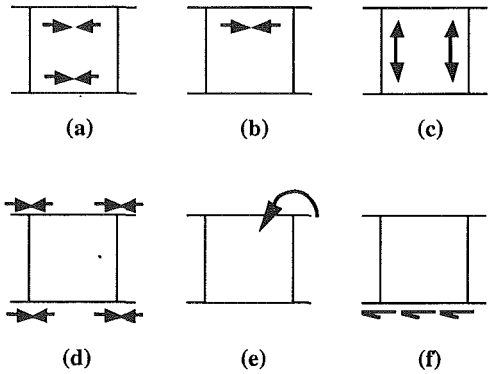

Fig. 2 Some force systems that may be equivalent in a cell sheet. (*a*) A distribution of microfilaments on both sides of the sheet. (*b*) Microfilaments on one side of the sheet. (*c*) Elongation of paraxially oriented microtubules. (*d*) Inter-cellular adhesions. (*e*) Oriented intercalation of cells. (*f*) Forces between the epithelial layer and its subjacent layer.

In addition, desmosomes and other kinds of junctional complexes occur between cells. These may be critical to normal development, in that they allow force transmission from cell to cell. Whether or not they otherwise affect morphogenesis, by actively driving cell rearrangement, for example, is not known.

Mechanical Equivalence

The sub-cellular actions of various cytoskeletal components and other force-generating structures may be quite different. However, at a cellular level their actions may be indistinguishable.

Equivalent Forces. The notion of equivalent systems of forces is well established in statics. It is also inherent in finite element analyses, where any of a wide variety of loads may give rise to the same equivalent joint loads. Any loads which give rise to the same equivalent joint loads would produce the same nodal displacements.

In embryology, it is often possible to observe the occurrence of a morphogenetic movement but not to know which of several possible forces drive the shape change. One is therefore faced with the inverse problem: determine the combination of forces which produce a particular sequence of displacements. In that case it would not be possible to distinguish between members of the set of applied forces which give rise to the same equivalent joint load vector. What constitutes a set of equivalent forces will depend on the scale of the model, the magnitude of the strains, and the boundary conditions.

A number of different force-generating mechanisms (some may be hypothetical) would tend to make a sheet which is constrained to move in-plane, without bending, narrow in the x-direction (Fig. 2):

(a) A distribution of microfilaments which produce components of force in the x-direction, on both sides of the sheet;

(b) A similar distribution of microfilaments on only one side of the sheet;

(c) Cells which maintain constant volume while paraxially-oriented microtubules in them elongate;

(d) Cells which maintain constant volume and are subject to adhesions between adjacent cells;

(e) Preferential intercalation of cells with neighbors which lie in the x-direction.

(f) Appropriately directed forces between the epithelial layer and its subjacent layer.

This is not an exhaustive list. Even if all six components of the stress and strain tensors could be ascertained, enough information would not, in general, be known to determine the relative contribution of each of a variety of possible force-generating mechanisms to that specific deformation.

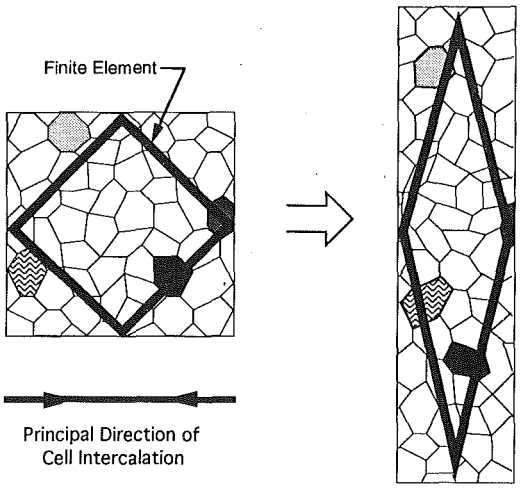

Fig. 3 Directed cell intercalation and corresponding finite element deformation

Equivalent Deformations. When a sheet or mass of cells undergoes a sequence of morphogenetic deformations, discrete processes are, presumably, involved as cells change neighbors and as individual atoms, molecules, monomers and filaments in each of the various cytoskeletal structures rearrange. Current computer limitations make it impractical to model even the discrete cellular behavior of typical morphogenetic movements, since several tens of thousands of cells are often actively involved. It then becomes useful to define sets of equivalent deformations as those patterns of local shape change which give rise to the same nodal displacements.

An examination of typical cell displacements during amphibian neurulation, a process which has been studied in some detail, shows that the displacement fields are surprisingly smooth and similar from embryo to embryo (Burnside and Jacobson, 1968). The regularity of these displacement fields suggests that they might be adequately modelled by continuum-based approaches like the finite element method. It must be recognized, however, that such a continuum model may not adequately model the forces produced by certain discrete processes.

That differences in inter-cellular adhesions exist and that they can drive cell rearrangements was demonstrated by Phillips and Steinberg (1978). They demonstrated that their aggregating cell masses behaved like viscous (fluid) continua. Forces generated by these differential adhesions have been postulated as a driving force in morphogenesis (Nardi, 1981). Simulations now exist which support this hypothesis (Weliky and Oster, 1990). When directed intercalations occur within a cell sheet or group of cells they will cause the sheet to narrow and elongate (Keller and Tibbetts, 1989; Keller et al., 1989; Weliky et al., 1991). Here, we approximate the effect of cell neighbor changes as a viscous continuum phenomenon.

A rectangular patch of cells is shown in Fig. 3. The principal direction of cell intercalation is indicated. An initially square finite element which might be used to model part of the patch is also shown. As the cell patch narrows and elongates, the element kinematically "conforms" to the bulk deformation. Irregularities in the displacement field caused by local effects associated with discrete neighbor changes are ignored in a continuum formulation.

Finite Element Formulation

The simulation of developmental shape changes poses a number of special challenges (Brodland, 1994). This is in part because large strains and large deflections occur. It is only recently that numerical implementations of the relevant theory (Brodland and Cohen, 1987; Peraire et al., 1988) have made simulations of organogenesis based on large-strain theory feasible. Analysis of biological systems is further complicated by the complex mechanical properties exhibited by cytoskeletal components.

Criteria. Certain criteria must be satisfied by a finite element formulation if it is to accurately model a substantial range of morphogenetic processes. Unlike many nonlinear problems of current interest, morphogenetic problems need not include inertial forces, in general (Odell et al., 1981). Furthermore, since most embryos have a density which matches closely the density of the medium in which they develop, gravitational effects can normally also be neglected. To accurately model typical morphogenetic mechanical behaviors the formulation must, however, include the following: temporal shape changes, changes of properties with time, three dimensional interactions, large deflections, large rotations (up to nearly 180 degrees during neurulation), large strains (up to 1000 percent (Burnside and Jacobson, 1968)), nonlinear material properties, material incompressibility (i.e., constancy of volume (Keeton and Gould, 1986)), and internal force generation. A commercial finite element package capable of satisfying these criteria could not be found.

Basic Formulation. The finite element formulation developed here is written in terms of an inertial, Cartesian reference frame. The occurrence of material nonlinearities, geometric nonlinearities, and rate-dependent material properties requires a formulation which is incremental through time. An explicit, stiffness formulation was chosen. In an explicit formulation like this, time steps must be chosen small enough to maintain solution stability.

The formulation and its implementation have been verified using standard methods including the patch test on slightly- and severely-deformed elements, comparison to basic large-strain, large-deflection and viscoelastic problems for which analytical solutions exist, and comparison of linear solutions with the commercial finite element package Modstar (Structural Research and Analysis Corporation, Santa Monica, CA). The patch tests indicate that quadrilateral elements based on the above formulation remain stable until and including when they become three-sided.

Volume Elements. Eight-noded isoparametric volume elements are used to represent volumetric components such as cell cytoplasm and to model the bulk properties of groups of cells. The derivation of the stiffness matrix for an isotropic elastic, 8-noded isoparametric volume element is reported in standard finite element texts (Huebner and Thornton, 1982; Zienkiewicz and Taylor, 1989). Nodal forces $\mathbf{f}$, for a Voigt viscoelastic element are given in terms of total and incremental nodal displacements, $\mathbf{u}$ and $\Delta\mathbf{u}$, by

$$\mathbf{f} = \mathbf{f}_E + \mathbf{f}_V = G\overline{\mathbf{K}}\mathbf{u} + \frac{\mu}{\Delta t}\overline{\mathbf{K}}\Delta\mathbf{u}. \tag{2}$$

where subscripts E and V denote the elastic and viscous components in terms of material shear modulus, G, and viscosity, μ. Since deformations are constant-volume, both the elastic and viscous components of the deformation can be represented using the same $\overline{\mathbf{K}}$ matrix. For an incremental change in position, $\Delta\mathbf{u}$, over a time step, Δt, we approximate $\dot{\mathbf{u}}$ by $\Delta\mathbf{u}/\Delta t$.

The elastic part at the kth step can be decomposed into its incremental components to give

$$\mathbf{f}_E = G\overline{\mathbf{K}}\Delta\mathbf{u} + \mathbf{r}. \tag{3}$$

where

$$\mathbf{r} = \sum_{j=0}^{k-1} G^j \overline{\mathbf{K}}^j \Delta\mathbf{u}^j, \tag{4}$$

represents the elemental restoring force vector for that single

Voigt element. For clarity, superscripts to denote the current (kth) step, where applicable, have been omitted.

When n Voigt models are placed in series, each carries the same force, $\mathbf{f}$, and the total displacement, $\Delta\mathbf{u}$, of the n Voigt models is

$$\Delta\mathbf{u} = \sum_{i=1}^{n} \Delta\mathbf{u}_i, \tag{5}$$

so that

$$\overline{\mathbf{K}}\Delta\mathbf{u} = \sum_{i=1}^{n} \frac{1}{G_i + \dfrac{\mu_i}{\Delta t}} (\mathbf{f} - \mathbf{r}_i) \tag{6}$$

To avoid storing the entire strain history of the element and to avoid stiffness matrix reevaluation using Eq. (6), we update the quantity $\mathbf{r}_i$, noting that its change during the most recent time step is

$$G_i\overline{\mathbf{K}}\Delta\mathbf{u}_i = \frac{G_i}{G_i + \dfrac{\mu_i}{\Delta t}} \left(\mathbf{f} - \sum_{j=0}^{k-1} G_i^j \overline{\mathbf{K}}_i^j \Delta\mathbf{u}_i^j\right). \tag{7}$$

Maintenance of volume constancy poses a number of technical challenges. In particular, full Gauss quadrature cannot be used, because it gives rise to numerical difficulties and locking (Belytschko and Ong, 1984). Reduction of the integration order to eliminate locking can result in spurious hourglass deformations. Here, reduced order integration is used and hourglassing is controlled using the technique devised by Liu et al. (1985). A further advantage of single point quadrature is that, compared to standard methods, it allows elements to undergo more severe shape changes before it becomes inaccurate.

Truss Elements. Truss finite elements are used to model subcellular components such as microfilaments, and microtubules. Like Hart and Trainor (1990) and Clausi and Brodland (1993), the mechanical effects of apical microtubules and microfilaments are modelled together.

Simulations

The above formulation makes it possible to investigate aspects of invagination, wave propagation, pattern formation, and neurulation. Volume elements are chosen to be approximately the same size as the epithelial cells they model. During many biological processes, such as gastrulation and eye formation, fluid and cells are contained beneath the epithelial sheet. Volume finite elements representing this subjacent material are assigned stiffnesses which are one percent of that of the top (epithelial) layer, unless noted otherwise. These elements, therefore, serve primarily to enforce constancy of volume in the region beneath the epithelium.

Truss elements are placed around the apical boundary of the cell. Initially, each is assigned negligible stiffness. To prevent the contraction force given by Eq. (1) from increasing without bound, we make each truss element stiff when it reaches its maximum physiological construction (Burnside, 1973).

Microfilament driving forces are characterized by a dimensionless parameter

$$F_A = \frac{N_{MF}F_{MF}}{\mu w h \theta}. \tag{8}$$

Here, N_{MF} is the effective number of microfilament bundles which act across a finite element volume which has initial width w and height h. The force produced by each microfilament bundle is F_{MF}, and θ is an inverse time parameter which relates dimensionless time, τ, to real developmental time, t, by

$$\theta = \frac{\tau}{t}. \tag{9}$$

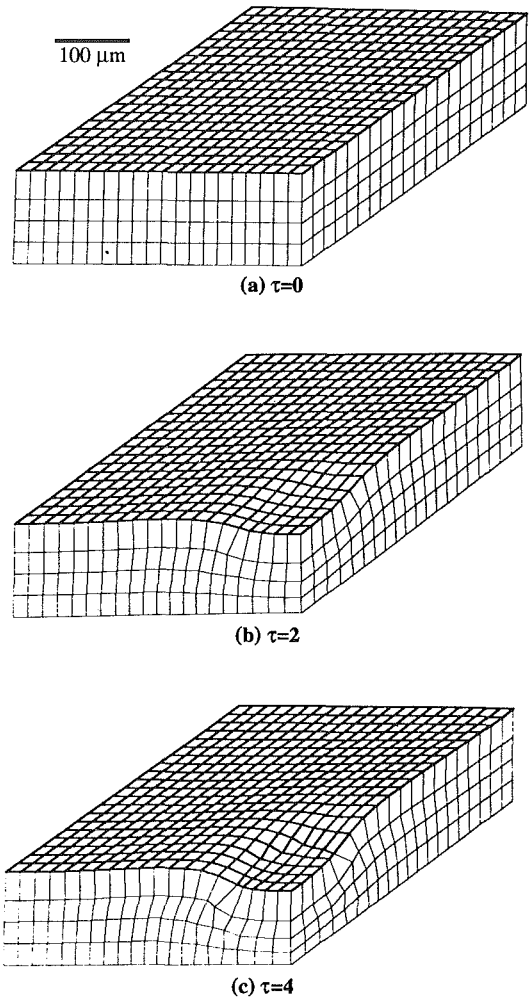

Fig. 4 Invagination on the surface of a tissue mass. One quarter of a large bi-symmetric patch of tissue is shown. Apical microfilaments act over the 5 by 5 patch of epithelial cells at the right front corner.

In each of the simulations presented here, $F_A = 0.10$.

Invagination. Invagination, the formation of a small pocket in an initially flat sheet of tissue, is essential to a wide variety of morphogenetic processes (Alberts et al., 1989). The most well known of these are gastrulation and optic cup formation. In most instances of invagination, the shape changes which occur appear axisymmetric with respect to the center of the initial depression.

We have identified only one previous simulation of invagination—a two-dimensional (planar) simulation of invagination and gastrulation (Odell et al., 1981). The planar analysis presented there demonstrates principal features of this basically axisymmetric process. As a caution, however, we note that especially when deflections are large, fully three-dimensional analyses may also identify different behaviors than planar or axisymmetric analyses (Bushnell, 1967; Brodland and Cohen, 1987).

Here, we perform a three-dimensional analysis of invagination. Because of the symmetry of the geometry and loading, we assume that it is sufficient to model one quarter of the cell sheet (Fig. 4). Each element in the top layer is initially 20 by 20 by 30 μm. Microfilaments act at the apical surface of the five by five patch of volume elements which is at the front right corner of the model region. Twenty time steps of $\Delta\tau = 0.2$ were used. Steps corresponding to $\tau = 0$, 2.0, and 4.0 are shown.

The invagination is produced by differences in the apical tensions which act on the cells inside the circle and those that

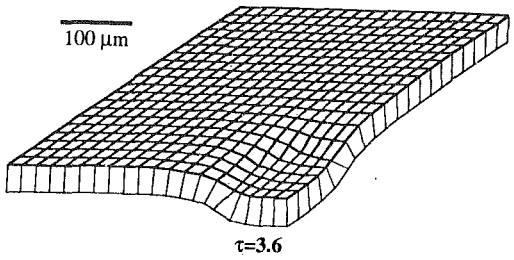

Fig. 5 Invagination of a sheet that has no subjacent material. The pattern of deformation is almost the same as that shown in Fig. 4. Corresponding degrees of deformation are produced somewhat more quickly in the sheet (e.g., $\tau = 3.6$ compared to $\tau = 4.0$).

act over the balance of the plate. Initially, a force imbalance between neighboring cells exists only at the boundary between the regions. The contractile force on the cells just inside the boundary is greater than that opposing it from the cells outside the boundary. The apical ends of these epithelial cells constrict and they become keystone-shaped. The part of the sheet which they form curves upwards. To maintain continuity, the epithelium just outside the boundary must curve downwards. In this way, an ogee profile is produced by a boundary layer phenomenon at the junction between the two regions. As the invagination continues to develop, a sharp depression with a relatively flat bottom is produced. Away from the boundary, the apical forces are balanced and the plate remains flat. It does, however, undergo significant in-plane contraction in the center. Since the edges of the plate are clamped, the outside of the plate is forced to undergo moderate dilation. A small amount of hourglass-like deformation is apparent in Fig. 4(*c*) even though full hourglass control is used. Apparently, the control proposed by Liu et al. (1985) is not totally effective under the strain field encountered here.

Based on the shape of the invagination produced by this simulation, we infer that the trapped cells might have little mechanical effect. A simulation of the epithelium alone supports this hypothesis (Fig. 5). The time step shown has an invagination of similar depth to that shown in Fig. 4(*c*). When underlying layers are present, their non-zero viscosity somewhat slows the shape changes. Their volume constancy also forces the plate to take a higher energy profile which, when the same driving forces act on a viscous system, further slows invagination. This simulation confirms that pressure from trapped material, present in the simulation shown in Fig. 4 is not the cause of the plate center remaining flat.

According to the Alfrey-McHenry analogy, identical displacement steps should be produced in a completely elastic system by a series of incremental forces which satisfy the relationship

$$\Delta \mathbf{f} = \frac{G\Delta t}{\mu}\,\mathbf{f}. \tag{10}$$

Computer simulations (not shown) for the single-layer geometry support this hypothesis. Other simulations demonstrate that when volume elements are represented using single viscoelastic Voigt elements, the mesh returns to its original configuration when microfilament forces are switched off.

Nardi (1981) argues that invaginations can be produced by intercellular adhesions. Simulations by Clausi and Brodland (1993), however, indicate that intercellular adhesions are not a primary driving force for invagination.

Wave Propagation. A variety of waves are known to propagate through embryonic cell sheets (Ready et al., 1976; Stern and Goodwin, 1977; Jacobson, 1978; Tomlinson, 1988; Brodland et al., 1994). The velocities of propagation vary widely, as do the apparent functions of the waves.

Figure 6(*a*) shows the initial, undeformed mesh used for the

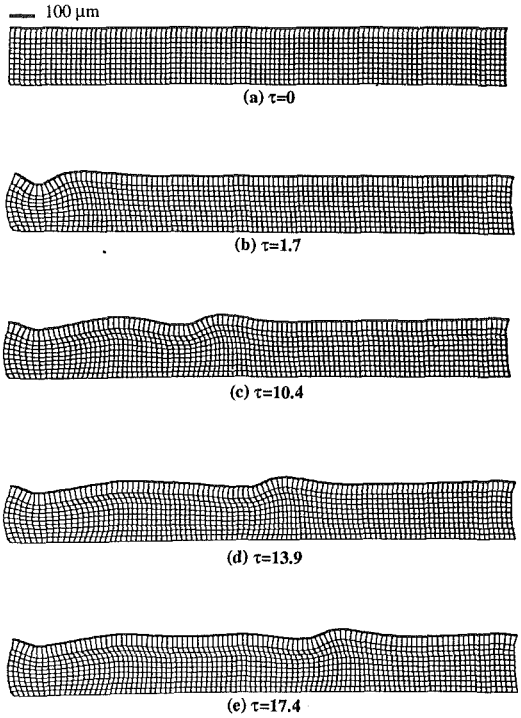

Fig. 6 Simulation of wave propagation. Stretch-induced contractions are activated sequentially. A furrowing contraction wave is produced.

simulation of wave propagation. This mesh represents a cross section of a sheet of cells. The top layer is composed of 20 by 20 by 40 μm tall elements which represent one cell each. In some cases, loose cells underlie the epithelium through which the contraction waves propagates. Nine layers of 20 by 20 by 20 μm elements represent this subjacent material. No tonus is used.

To initiate the wave, a small group of cells close to the left edge are made to contract until a dimple is produced (Fig. 6(*b*)). Stretch activated contractions are required to sustain wave propagation, since the medium has a viscous component, and the wave would otherwise decay. The wave shown propagating in Figs. 6(*c*) to (*e*) was established by manually triggering, in sequence, stretch activated contractions of magnitude $F_A = 0.10$ and duration $\tau = 0.90$ at each time step of $\Delta\tau = 0.30$. The wave propagates at a velocity of 69 $\mu\text{m}\cdot\theta$. Other simulations (not shown), suggest that, in general, a wave initiated this way can change shape significantly as it propagates until it achieves a stable profile.

The strain rate at the apex of the epithelial cell immediately ahead of those which are actively constricting increases sharply to 0.023. This is an increase of 24 percent compared to the previous time step. Simultaneously, the strain rate in these cells increases sharply by 36 percent to $0.18\cdot\theta$. This suggests that either of these criteria might be used to trigger subsequent stretch activated contractions. The biological literature suggests that it is stretching of the apical membrane which normally initiates microfilament contraction. Because these quantities increase sharply, a wave triggered by this means would exhibit considerable stability.

In the simulation shown, no elastic forces are present to assist in restoration of the original mesh geometry. Thus, the almost complete restoration of the rectangular geometries of both the top and underlying layers as the wave passes is due entirely to forces produced by the wave.

In an epithelium, the cytoplasm is partitioned into small volumes by the cell membranes. Thus, localized apical constrictions associated with a wave cause individual cells to become keystone shaped as their cytoplasm is forced to their

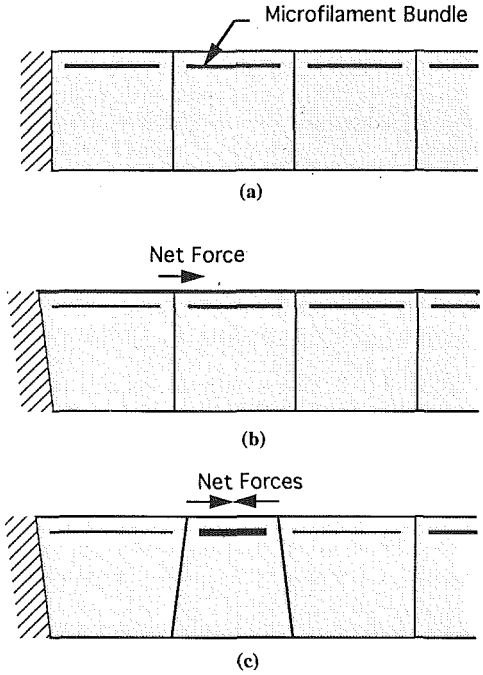

Fig. 7 Mechanical pattern formation. Because the force produced by an individual microfilament bundle decreases as its length increases, a mechanical instability can occur. A small perturbation initiates the formation of a sequence of alternating stretched and shortened microfilaments, i.e., pattern.

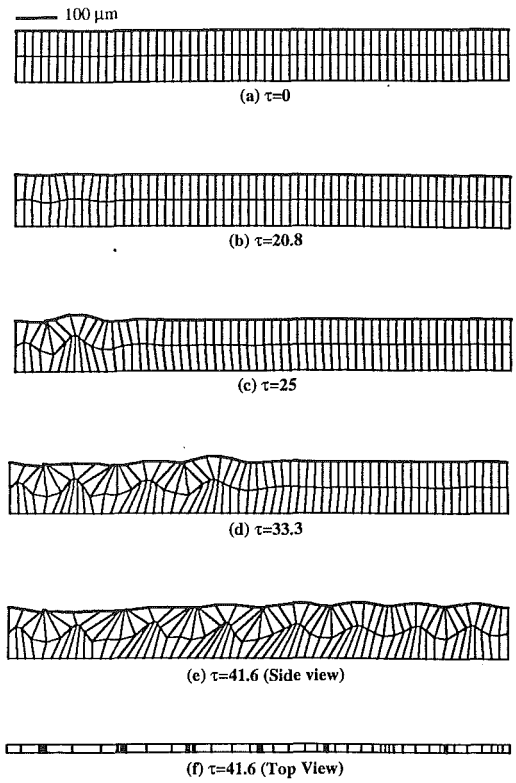

Fig. 8 Simulation of mechanical pattern formation. Pattern is initiated by a manually applied perturbation at the left edge. Spontaneous initiation of pattern from the right side is just visible in part (*d*) of the figure.

basal end. Thus, a propagating dimple or furrow is produced. In fertilized eggs, the cytoplasm is not partitioned by cell membranes and contraction waves which propagate over fertilized eggs do not, apparently, produce furrowing.

Pattern Formation. Pattern formation, a process by which an initially homogeneous collection of cells develops heterogeneous features, is another critical embryonic process which has received much attention. Not only is it responsible for the establishment of surface features and coloration, but numerous internal structures as well. In vertebrate development, it establishes the location and number of somites and, thus, corresponding principal features of the vertebral column. Later, it directs the patterns of mesenchyme cell condensation and thus determines numerous features of limb segmentation and internal structure (Maini and Solursh, 1991).

A variety of models have been proposed to explain aspects of pattern formation. These include models based on gradients or reaction-diffusion (Turing models) of biochemical morphogens, triggering of events by the advancement of a progress zone, and differential adhesion models. For a review, see Miani and Solursh (1991).

Both biochemical changes and mechanical events are involved in most pattern formation processes. In many cases it is not clear whether the initial stage of the process is mechanical or biochemical. The initial event may vary from species to species or from one pattern formation process to another. It is known that in some cases mechanical changes precede biochemical differentiation (Althouse and Solursh, 1987). Experiments by Ben Ze'ev (1985) which demonstrate that specific protein synthesis can be caused by changes in cell shape support this observation.

Here, we demonstrate that pattern formation might occur in epithelial sheets solely as a result of microfilament contraction. Consider the cell sheet cross section shown in Fig. 7(*a*). Now, suppose that a perturbation, such as the lateral displacement shown, occurs. Initially, this causes the width of one cell to be reduced (Fig. 7(*b*)). The load carrying capacity of the microfilament bundle at the apical end of that cell will be increased as it shortens. The bundle in the neighboring cell will not have a matching increased force. Thus, the shortened bundle will continue to shorten while the bundle in the neighboring cell will be stretched. In turn, this bundle will be out of balance with its other neighbor (Fig. 7(*c*)), and a propagating imbalance will produce a sequence of alternating states; i.e., pattern.

Figure 8 shows the results of a simulation of a strip of 20 by 20 by 60 μm cells. Part (*a*) of the figure shows the initial state. The top left node is initially displaced 1 μm to the left to provide a small perturbation and initiate pattern formation. The initial stages of deformation proceed in an exponentially increasing fashion until formation of the first dimple is approached. Parts (*b*) through (*e*) of the figure show the propagation of pattern formation. Relative times are given on the figure. The right edge of the sheet is fixed. Since pattern formation here results from a mechanical instability, it is not surprising that pattern formation also initiates eventually from the right edge. The initial stages of this process are just discernable in Fig. 8(*d*).

Figure 8(*f*) shows a top view of the sheet shown in Fig. 8(*e*). In general, it would be this surface which could be observed. A stripe-like pattern is evident. The stripes are well established at the left side, while the most recently formed stripe, the sixth one from the left, is not as well defined. As the simulation continues (not shown), all stripes became equally well defined.

Figure 9 shows the results of a parametric analysis of mechanical pattern formation. The spatial distribution of the patterns is shown. In all cases, the pattern spacing is regular. Times of formation are not shown. Doubling the width of the elements has little effect. Increasing the viscosity of the bottom layer by a factor of 100 so that it matches the top layer has little effect on pattern spacing but slows the rate of pattern formation by approximately 20 percent. Making the top layer half as thick reduces the spacing of the patterns by approximately 30 percent and increase the time required to form them

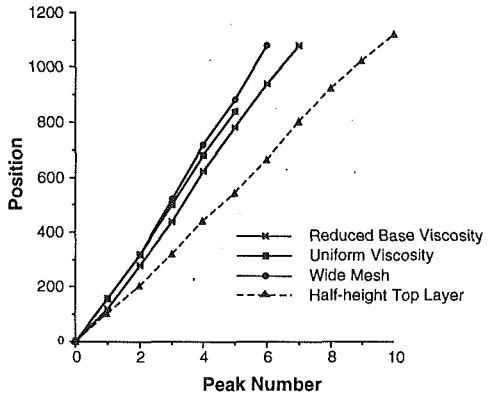

Fig. 9 Effect of parameters on pattern spacing. Subjacent layer properties have little effect on the spacing of the pattern, but affect its rate of formation. Epithelium thickness affects both spacing and rate of pattern formation.

by a factor of nearly three. In general, the pattern cycle is wider than two cells, and not as implied by Fig. 7.

Pattern formation by the mechanical means demonstrated here is, unlike some other models (Maini and Solursh, 1991), highly robust. Pattern spacing and rate of formation are largely unaffected by cell size and subjacent layer stiffness. Patterns produced in thin epithelia by this means are more closely spaced.

Neurulation. Neurulation, a morphogenetic process during which a sheet of tissue called the neural plate reshapes itself and rolls up to form a closed tube, has been studied extensively. The principal mechanical steps in the process are described elsewhere (Gordon and Brodland, 1989; Schoenwolf and Smith, 1990).

Three primary theories exist to account for the observed shape changes. The classical view is that the apical microfilaments of epithelial cells constrict to cause the shape changes. (Baker and Schroeder, 1967; Burnside, 1971, 1973). To account for observed shearing deformations which occur at the neural ridges, Jacobson et al. (1986) have proposed a cortical tractor model. Both of these models are based on the notion that the forces which shape the neural plate are produced within the plate. In contrast, Smith and Schoenwolf (1991) have argued that forces extrinsic to the neural plate may also act.

Evidence that intrinsic forces are sufficient to cause neural tube closure exists (Jacobson and Gordon, 1976; Lee and Nagele, 1988) as does evidence that extrinsic forces are involved (Smith and Schoenwolf, 1991). Much puzzling and apparently contradictory evidence exists. Two plausible explanations exist from these apparent paradoxes. It may be that redundancy exists between the various forces which shape the neural tube. It may also be that fundamental differences exist in the mechanisms of neural tube closure from one species to another (Clausi and Brodland, 1993).

Since neurulation is such an important morphogenetic process, it is not surprising that numerous computer simulations of parts of the neurulation process have been done (Jacobson and Gordon, 1976; Odell et al., 1981; Jacobson et al., 1986; Clausi, 1991). Jacobson and Gordon (1976) used systems of contacting circular elements to investigate the in-plane motions which accompany neural plate reshaping. In their kinematic model, both pre-programmed changes in element diameter and neighbor changes are required to produce observed shape changes. Odell et al. (1981) developed a two-dimensional model of cell behavior based on hypothetical, multi-parameter mechanical components which run along the sides and diagonals of quadrilateral elements. By varying geometric and material parameter values, they are able to simulate a variety of phenomena including neural tube closure. The Odell et al. model has been used by Dunnett et al. (1991) to demonstrate the possible mechanical roles of various alterations in mechanical properties in the causation of neural tube defects. We note that the ratio of cell heights to embryo diameter they use are quite different from those used by Odell et al. in their original simulations.

Since neurulation is symmetrical about the center plane of the embryo, we model only the right half of the embryo. Cells which are 20 by 20 by 60 μm are used. We assume that apical contractions alone drive the shape changes. The right edge of the sheet is clamped.

The resulting sequence of shape changes has several noteworthy features which correspond to typical embryo development:

1 Initially all cells have similar geometries (Fig. 10(*a*)).
2 Distinct, asymmetrical ridges appear early (Fig. 10(*b*)).
3 The neural plate narrows and thickens while the epidermis expands and thins.
4 A depression (neural groove) forms at the midline (Fig. 10(*c*)).
5 As the neural ridge develops, cells near its root skew significantly. (Jacobson et al., 1986; Brodland and Shu, 1992).
6 Another feature of neural tube closure which is evident in many species is the formation of what Schoenwolf calls "hinges" at the midline of the neural plant and at locations approximately two-thirds of the way towards the edge of the neural plate (Schoenwolf and Smith, 1990) (Fig. 8(*c*)). These are narrow regions of the neural plate where distinctly higher curvatures develop compared to adjacent regions. We are not aware that any previous simulations of neurulation contain evidence of hinges, and we did not anticipate that our simulations would produce these curious features.

We recognize that this simulation has several shortcomings. The most evident is that the neural tube does not close. The early stages of neurulation are concurrent with the final stages of gastrulation. It is, thus, possible that the tension of the epidermis decreases during the latter stages of neurulation. The simulation shown in Fig. 11 is the same as that shown in Fig. 10, except that the lateral edge of the epidermis is allowed to move inwards at a rate of 36 $\mu m \cdot \theta$. In this case, the neural tube closes. Because of the substantial shape changes which occur during neurulation, simulations of this process require many more time steps (typically 500) than the other simulations, which require less than 60 time steps.

The simulations of neural tube formation presented here demonstrate that numerous features of neurulation, including several not previously demonstrated using simulations, can be produced by apical constriction alone. Specifically, cell skewing at the root of the neural ridges and "hinge" formation may not, in fact, require the action of other mechanisms. Both of these phenomena occurred in our earliest simulations and were unexpected. Cell skewing in these simulations is the result of shearing forces carried by the plate. The specific mechanical cause of the hinges is still not entirely clear. It may be the result of an instability akin to that which causes pattern formation. Unfortunately, the results are not directly comparable with force measurement made by Selman (1958).

Simulations by Clausi and Brodland (1993), have shown that changes to the initial thickness of the epithelial cell sheet can significantly affect the shape changes which are produced. Elongation of the neural plate in the direction normal to the plane of the simulations normally accompany neurulation and may be important mechanically. Finally, we note that significant species-to-species variations exist in neurulation geometries. For example, amphibian neurulation occurs on a spherically-shaped surface while neurulation in birds and mammals occurs on a basically planar surface, as implied by the simulations presented here. Somewhat different cross-sectons are produced.

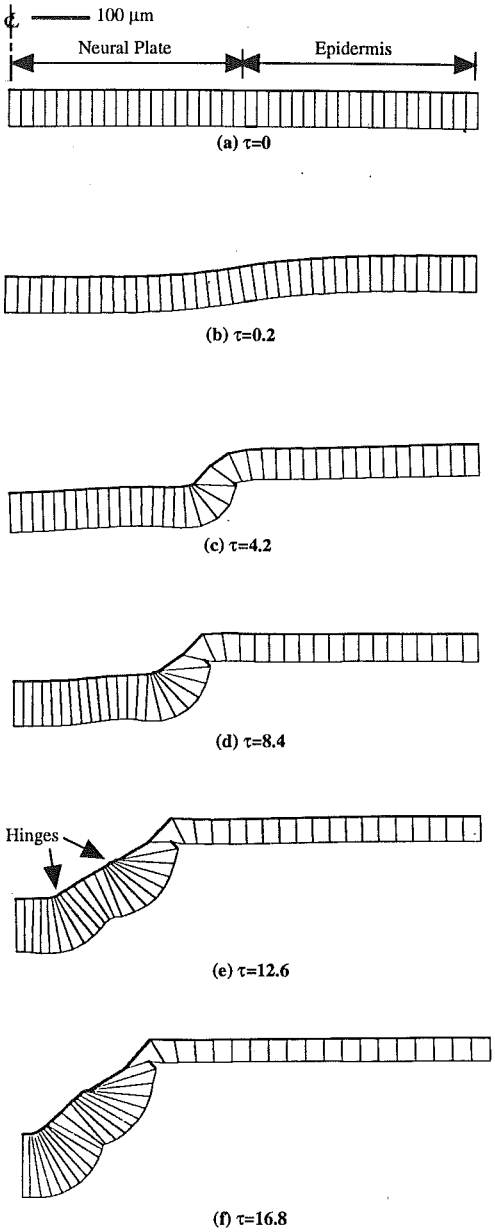

Fig. 10 Neurulation—right edge fixed. The right half of the epithelium of the embryo is shown. (*a*) Initial state. (*b*) and (*c*) Formation of neural ridge. (*d*) Narrowing of plate. (*e*) and (*f*) Hinge formation. A closed tube does not form.

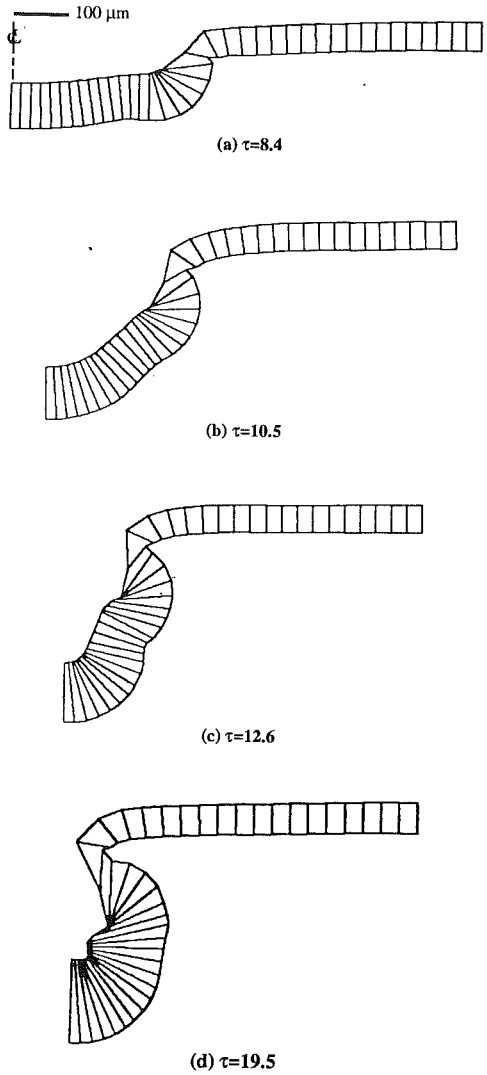

Fig. 11 Neurulation—right edge moves inward. (*a*) Similar to 10(*d*). (*b*) and (*c*) Hinge formation and substantial progress toward the formation of a tube. (*d*) Tube closure.

Discussion

A variety of physical phenomena are manifested by developing embyros. These include mechanical forces, electric fields and biochemical signals (Jaffe, 1979; Alberts et al., 1989). The specific role and possible importance of some of these is still unclear. Recent experiments (Ben-Ze'ev, 1985) have suggested that these interactions may be even more complex than previously thought and that mechanical changes can trigger biochemical changes. It is self-evident, however, that mechanical forces are crucial to morphogenetic shape changes in embryronic tissues, since they alone can drive these shape changes. Even though many biological phenomena have been studied extensively from a biochemical point of view, mechanical analyses are conspicuously rare. The purpose of this paper has been to demonstrate possible mechanical bases for some of these phenomena; namely, invagination, wave propagation, pattern formation and neurulation. Detailed comparisons with the large body of biological data are beyond the scope of this work. We note that a wide variety of mechanical phenomena are produced by a surprisingly small set of force generators. It should perhaps not be surprising, therefore, that apparently different phenomena occur together (Stern and Goodwin, 1977; Jacobson, 1978).

Extensive and complex biochemical processes, some of which are initiated from hierarchical levels as high as the nucleus of the cell, undoubtedly play a crucial role as well. It is known, for example, that they initiate and control the design and construction of sophisticated force producing structures, regulate their mechanical action, and govern their disassembly (Alberts et al., 1989). This notwithstanding, it is evident that the end effector for morphogenetic shape changes is mechanical.

Within this framework, mechanical simulations serve an important purpose. They make it possible to test whether or not specific systems of mechanical forces can produce observed patterns of shape change. To prove that specific kinds of mechanical forces alone are not sufficient to produce a certain phenomenon is more difficult. A detailed parametric study which spans the domain of possible combinations of forces is required and all simulations in the set must give negative results.

Simulations allow specific hypothesis about these processes to be tested, and make it possible to investigate "what if"

questions. It is not possible, in general, to answer such questions by experiments because subtle changes are difficult if not impossible to make and possible subsidiary effects of drugs and teratogens are difficult to identify. The notions of equivalent forces and equivalent actions set limits on what can be ascertained from simulations.

The finite element formulation presented here has proved effective in modeling a variety of mechanical morphogenetic processes. Entirely mechanical bases for invagination, contraction wave propagation, pattern formation and neurulation have been demonstrated. Limited parametric analyses have made it possible to identify some geometric and material properties which are essential to specific phenomena and some which are not. The simulations suggest a number of possible physical experiments.

Acknowledgments

This research was funded by the Easter Seal Research Institute of Ontario and the Natural Sciences and Engineering Research Council of Canada (NSERC).

References

Alberts, B., Bray, D., Lewis, J., Raff, M., Roberts, K., Watson, J., 1989, *Molecular Biology of the Cell*, 2nd ed., Garland Publishing, Inc., New York.

Albrecht-Buehler, G., 1990, "In Defense of 'Nonmolecular' Cell Biology," *International Review of Cytology*, Vol. 120, pp. 191–241.

Aulthouse, A. L., and M. Solursh, 1987, "The Detection of a Precartilage Blastema-Specific Maker," *Dev. Biol.*, Vol. 120, pp. 377–384.

Baker, P. C., and Schroeder, T. E., 1967, "Cytoplasmic Filaments and Morphogenetic Movements in the Amphibian Neural Tube," *Dev. Biol.*, Vol. 15, pp. 432–450.

Belytschko, T., Ong, J. S., 1984, "Hourglass in Linear and Nonlinear Problems," *Comp. Meth. in Appl. Mech. and Eng.*, Vol. 43, pp. 251–276.

Ben-Ze'ev, A., 1985, "Cell-Cell Interaction and Cell Configuration-Related Control of Cytokeratins and Vimentin Expression in Epithelial Cells and in Fibroblasts," *Ann N.Y. Acad. Sci.*, Vol. 455, pp. 597–613.

Brodland, G. W., 1994, "Finite Element Methods for Developmental Biology," *International Review of Cytology*, Vol. 150, pp. 95–118.

Brodland, G. W., and Cohen, H., 1989, "Deflection and Snapping of Ring-Loaded Spherical Caps," ASME *J. Appl. Mech.*, Vol. 111, No. 56, pp. 127–132.

Brodland, G. W., and Gordon, R., 1990, "Intermediate Filaments May Prevent Buckling of Compressively Loaded Microtubules," ASME JOURNAL OF BIOMECHANICAL ENGINEERING, Vol. 112, pp. 319–321.

Brodland, G. W., and Shu, D-W., 1992, "Are Intercellular Membrane Forces Important to Amphibian Neurulation?" *Dynamical Phenomena at Interfaces, Surfaces and Membranes*, G. Forgacs and D. Beysens, eds., Nova Science Publishers, New York, pp. 237–245.

Brodland, G. W., Gordon, R., Scott, M. J., Björklund, N. K., Luchka, K. B., Martin, C. C., Matuga, C., Globus, M., Vethamany-Globus, S., and Shu, D., 1994, "Furrowing Surface Contraction Wave Coincident with Primary Neural Induction in Amphibian Embryos," *J. Morphology*, Vol. 219, pp. 131–142.

Burnside, B., 1971, "Microtubules and Microfilaments in Newt Neurulation," *Dev. Biol.*, Vol. 26, pp. 416–441.

Burnside, B., 1973, "Microtubules and Microfilaments in Amphibian Neurulation," *Amer. Zool.*, Vol. 13, pp. 989–1006.

Burnside, M. B., and Jacobson, A. G., 1968, "Analysis of Morphogenetic Movements in the Neural Plate of the Newt Taricha Torosa," *Dev. Biol.*, Vol. 18, pp. 537–552.

Bushnell, D., 1967, "Bifurcation Phenomena in Spherical Shells under Concentrated and Ring Loads," *AIAA Journal*, Vol. 5, No. 11, pp. 2034–2040.

Cassimeris, L., Pryer, N. K., and Salmon, E. D., 1988, "Real-Time Observations of Microtubule Dynamic Instability in Living Cells," *The Journal of Cell Biology*, Vol. 107, No. 6, pp 2223–2231.

Clausi, D. A., 1991, "Finite Element Simulations of Early Embryonic Development," M.A.Sc. thesis, University of Waterloo.

Clausi, D. A., and Brodland, G. W., 1993, "Mechanical Evaluation of Theories of Neurulation Using Computer Simulations," *Development*, Vol. 118, pp. 1013–1023.

Dunnett, D., Goodbody, A., and Stanisstreet, M., 1991, "Computer Modelling of Neural Tube Defects," *Acta Biotheoretica*, Vol. 39, pp. 63–79.

Dustin, P., 1984, *Microtubules*, 2nd ed. Springer-Verlag, Berlin.

Gordon, R., and Brodland, G. W., 1987, "The Cytoskeletal Mechanics of Brain Morphogenesis: Cell State Splitters and Primary Neural Induction," *Cells Biophys.*, Vol. 11, pp. 177–237.

Gordon, R., and Brodland, G. W., 1989, "Neurulation," *Developmental Biology of the Axolotl*, J. B. Armstrong and G. M. Malacinski, eds., Oxford University Press, New York.

Gordon, S. R., and Essner, E., 1987, "Investigations on Circumferential Microfilament Bundles in Rat Retinal Pigment Epithelium," *European Journal of Cell Biology*, Vol. 44, pp. 97–104.

Hart, T. N., and Trainor, L. E. H., 1990, "The Two-Component Model for the Cytoskeleton in Development," *Physica*, Vol. D44, pp. 269–284.

Hilfer, S. R., and Hilfer, E. S., 1983, "Computer Simulation of Organogenesis: An Approach to the Analysis of Shape Changes in Epithelial Organs," *Dev. Biol.*, Vol. 97, pp. 444–453.

Hill, T. L., 1981, "Microfilament or Microtubule Assembly or Disassembly Against a Force," *Proc. Natl. Acad. Sci.*, Vol. 78, No. 9, pp. 5613–5617.

Hill, T. L., and Kirschner, M. W., 1982a, "Subunit Treadmilling of Microtubules or Actin in the Presence of Cellular Barriers: Possible Conversion of Chemical Free Energy into Mechanical Work," *Proc. Natl. Acad. Sci. USA*, Vol. 79, pp. 490–494.

Hill, T. L., and Kirschner, M. W., 1982b, "Bioenergetics and Kinetics of Microtubules and Actin Filament Assembly-Disassembly," *Int. Rev. Cytol.*, Vol. 78, pp. 1–125.

Hiramoto, Y., 1969a, "Mechanical Properties of the Protoplasm of the Sea Urchin Egg: II. Unfertilized Egg," *Expl. Cell Res.*, Vol. 56, pp. 201–208.

Hiramoto, Y., 1969b, "Mechanical Properties of the Protoplasm of the Sea Urchin Egg: II. Fertilized Egg," *Expl. Cell Res.*, Vol. 56, pp. 209–218.

Horio, T., and Hotani, H., 1986, "Visualization of the Dynamic Instability of Individual Microtubules by Dark-Field Microscopy," *Nature*, Vol. 321.

Huebner, K. H., and Thornton, E. A., 1982, *The Finite Element Method for Engineers*, 2nd ed., John Wiley & Sons, Toronto.

Jacobson, A. G., and Gordon, R., 1976, "Changes in the Shape of the Developing Vertebrate Nervous System Analyzed Experimentally, Mathematically and by Computer Simulation," *J. Exp. Zool.*, Vol. 197, pp. 191–246.

Jacobson, A. G., 1978, "Some Forces that Shape the Nervous System," *Zoon*, Vol. 6, pp. 13–21.

Jacobson, A. G., 1980, "Computer Modelling of Morphogenesis," *Amer. Zool.*, Vol. 20, pp. 669–677.

Jacobson, A. G., Oster, G. F., Odell, G. M., and Cheng, L. Y., 1986, "Neurulation and the Cortical Tractoring Model for Epithelial Folding," *J. Embryol. Exp. Morph.*, Vol. 96, pp. 19–49.

Jaffe, L. F., 1979, "Strong Electrical Currents Leave the Primitive Streak of Chick Embryos," *Science*, Vol. 206, No. 2, pp. 569–571.

Keeton, W. T., and Gould, J. L., 1986, *Biological Science*, 4th ed., W. W. Norton and Company, New York.

Keller, R., and Tibbetts, P., 1989, "Mediolateral Cell Intercalation in the Dorsal Axial Mesoderm of Xenopus Iaevis," *Dev. Biol.*, Vol. 131, pp. 539–549.

Keller, R., Cooper, M. S., Danilchik, P. T., and Wilson, P. A., 1989, "Cell Intercalation During Notochord Development in Xenopus Iaevis," *J. of Expl. Zool.*, Vol. 251, pp. 134–154.

Koehl, M. A. R., 1990, "Biomechanical Approaches to Morphogenesis," *Seminars in Developmental Biology*, Vol. 1, pp. 367–378.

Lee, H-Y., and Nagele, R. G., 1985, "Studies on the Mechanisms of Neurulation in the Chick: Interrelationship of Contractile Proteins, Microfilaments, and the Shape of Neuroepithelial Cells," *J. of Expl. Biol.*, Vol. 235, pp. 205–215.

Lee, H., and Nagele, R. G., 1988, "Intrinsic Forces Alone are Sufficient to Cause Closure of the Neural Tube in the Chick," *Experientia*, Vol. 44, pp. 60–61.

Liu, W. K., Ong, J. S., and Uras, R. A., 1985, "Finite Element Stabilization Matrices—A Unification Approach," *Comp. Meth. in Appl. Mech. and Eng.*, Vol. 53, pp. 13–46.

Maini, P. K., and Solursh, M., 1991, "Cellular Mechanisms of Pattern Formation in the Developing Limb," *International Review of Cytology*, K. W. Jeon and M. Friedlander, eds., Vol. 129, pp. 91–133.

Mizushima-Sugano, J., Maeda, T., and Miki-Noumura, T., 1983, "Flexural Rigidity of Singlet Microtubules Estimated from Statistical Analysis of Their Contour Lengths and End-to-end Distances," *Biochimica et Biophysica Acta*, Vol. 755, No. 2, pp. 257–262.

Nakamura, S., and Hiramoto, Y., 1978, "Mechanical Properties of the Cell Surface in Starfish Eggs," *Develop., Growth and Differ.*, Vol. 20, No. 4, pp. 317–327.

Nardi, J. B., 1981, "Epithelial Invagination: Adhesive Properties of Cells can Govern Position and Directionality of Epithelial Folding," *Differentiation*, Vol. 20, pp. 97–103.

Odell, G. M., Oster, G., Alberch, P., and Burnside, B., 1981, "The Mechanical Basis of Morphogenesis, I. Epithelial Folding and Invagination," *Dev. Biol.*, Vol. 85, pp. 446–462.

Peraire, J., Peiro, J., Formaggia, L., Morgan, K., and Zienkiewicz, O. C., 1988, "Finite Element Euler Computations in Three Dimensions," *Int. J. Num. Meth. Eng.*, Vol. 26, pp. 2135–2159.

Phillips, H. M., and Steinberg, M. S., 1978, "Embryonic Tissues as Elastoviscous Liquids," *J. Cell. Sci.*, Vol. 30, pp. 1–20.

Rappaport, R., 1977, "Tensiometric Studies of Cytokinesis in Cleaving Sand Dollar Eggs," *J. Expl. Zool.*, Vol. 201, pp. 375–378.

Ready, D. F., Harson, T. E., and Benzer, S., 1976, "Development of the Drosophila Retina, a Neurocrystalline Lattice," *Dev. Biol.*, Vol. 53, pp. 217–240.

Regirer, S. A., 1989, "Active Media with Discrete Sources and 'Jumping Waves'," *Nonlinear Waves in Active Media*, J. Engelbrecht, ed., Springer-Verlag, Berlin, Heidelberg.

Sachs, F., 1990, "Stretch-Sensitive Ion Channels," *Seminars in The Neurosciences*, Vol. 2, pp. 49–57.

Schoenwolf, G. C., and Smith, J. L., 1990, "Mechanisms of Neurulation: Traditional Viewpoint and Recent Advances," *Development*, Vol. 109, pp. 243–270.

Selman, G. G., 1958, "The Forces Producing Neural Closure in Amphibia," *J. Embryol. Exp. Morph.*, Vol. 6, pp. 448–465.

Smith, J. L., and Schoenwolf, G. C., 1991, "Further Evidence of Extrinsic Forces in Bending of the Neural Plate," *The Journal of Comparative Neurology*, Vol. 307, pp. 225–236.

Stephens, N. L., editor, 1984, Smooth Muscle Contraction, Marcel Dekker, New York.

Stern, C. D., and Goodwind, B. C., 1977, "Waves and Periodic Events During Primitive Streak Formation in the Chick," *J. Embryol. Exp. Morph.*, Vol. 41, pp. 15–22.

Tomlinson, A., 1988, "Cellular Interactions in the Developing Drosophila Eye," *Development*, Vol. 104, pp. 183–193.

Valerg, P. A., and Alvertini, D. F., 1985, "Cytoplasmic Motions, Rheology, Structure Probed by a Novel Magnetic Particle Method," *J. Cell. Biol.*, Vol. 101, pp. 130–140.

Weliky, M., Minsuk, S., Keller, R., and Oster, G., 1991, "Notochord Morphogenesis in Xenopus Laevis: Simulation of Cell Behavior Underlying Tissue Convergence and Extension," *Development*, Vol. 113, pp. 1231–1244.

Weliky, M., and Oster, G., 1990, "The Mechanical Basis of Cell Rearrangement I. Epithelial Morphogenesis During Fundulus Epiboly," *Development*, Vol. 109, pp. 373–386.

Zienkiewicz, O. C., and Taylor, R. L., 1989, *The Finite Element Method*, Vol. 1, 4th ed., McGraw-Hill Book Company Limited, Toronto.